Targeting of KRAS mutant tumors by HSP90 inhibitors involves degradation of STK33

Ninel Azoitei,[1] Christopher M. Hoffmann,[4] Jana M. Ellegast,[1] Claudia R. Ball,[4] Kerstin Obermayer,[1] Ulrike Gößele,[1] Britta Koch,[1] Katrin Faber,[1] Felicitas Genze,[2] Mark Schrader,[2] Hans A. Kestler,[3] Hartmut Döhner,[1] Gabriela Chiosis,[5] Hanno Glimm,[4] Stefan Fröhling,[1] and Claudia Scholl[1]

[1]Department of Internal Medicine III, [2]Department of Urology, and [3]Institute for Neural Information Processing, Ulm University, 89081 Ulm, Germany
[4]Department of Translational Oncology, National Center for Tumor Diseases and German Cancer Research Center, 69120 Heidelberg, Germany
[5]Department of Molecular Pharmacology and Chemistry, Sloan-Kettering Institute, New York, NY 10065

Previous efforts to develop drugs that directly inhibit the activity of mutant *KRAS*, the most commonly mutated human oncogene, have not been successful. Cancer cells driven by mutant KRAS require expression of the serine/threonine kinase STK33 for their viability and proliferation, identifying STK33 as a context-dependent therapeutic target. However, specific strategies for interfering with the critical functions of STK33 are not yet available. Here, using a mass spectrometry-based screen for STK33 protein interaction partners, we report that the HSP90/CDC37 chaperone complex binds to and stabilizes STK33 in human cancer cells. Pharmacologic inhibition of HSP90, using structurally divergent small molecules currently in clinical development, induced proteasome-mediated degradation of STK33 in human cancer cells of various tissue origin in vitro and in vivo, and triggered apoptosis preferentially in KRAS mutant cells in an STK33-dependent manner. Furthermore, HSP90 inhibitor treatment impaired sphere formation and viability of primary human colon tumor-initiating cells harboring mutant KRAS. These findings provide mechanistic insight into the activity of HSP90 inhibitors in KRAS mutant cancer cells, indicate that the enhanced requirement for STK33 can be exploited to target mutant KRAS-driven tumors, and identify STK33 depletion through HSP90 inhibition as a biomarker-guided therapeutic strategy with immediate translational potential.

CORRESPONDENCE
Claudia Scholl:
claudia.scholl@uni-ulm.de
OR
Stefan Fröhling:
stefan.froehling@uni-ulm.de

Abbreviations used: AML, acute myeloid leukemia; CAM, chorioallantoic membrane; HA, hemagglutinin; IHC, immunohistochemistry; IP, immunoprecipitation; RNAi, RNA interference; shRNA, short hairpin RNA; TUNEL, terminal deoxynucleotidyl transferase dUTP nick end labeling.

In recent years, the focus of cancer drug development has shifted from conventional cytotoxic drugs to molecularly targeted therapeutics (de Bono and Ashworth, 2010). To achieve the goal of tailored, pathogenesis-oriented cancer therapies, detailed knowledge of the events that underlie the initiation and maintenance of the transformed phenotype is necessary (Stratton et al., 2009), an insight that has fueled major efforts to catalog the genetic changes that drive the most common human cancers (International Cancer Genome Consortium, 2010). However, even though the identification of acquired genetic alterations that cause certain cancer types has led to remarkable therapeutic successes (Hudis, 2007; Sharma et al., 2007; Druker, 2009), many cancer-associated mutations are difficult to inhibit directly. Thus, only a limited number of discoveries from current cancer genome efforts have generated immediately actionable drug targets.

The dilemma of "undruggable" genetic lesions is exemplified by the point mutations in the *KRAS* protooncogene that occur in ∼30% of human cancers and are particularly prevalent

C. Scholl and S. Fröhling contributed equally to this paper.

The Rockefeller University Press $30.00
J. Exp. Med. Vol. 209 No. 4 697-711
www.jem.org/cgi/doi/10.1084/jem.20111910

in adenocarcinomas of the pancreas, lung, and colon (Karnoub and Weinberg, 2008). Although oncogenic *KRAS* alleles were first identified >20 yr ago, mutant KRAS has evaded all attempts at therapeutic targeting so far (Malumbres and Barbacid, 2003; Downward, 2003; Roberts and Der, 2007). Furthermore, KRAS mutations have not only proved to be undruggable, but are now understood to be predictors of nonresponsiveness to molecularly targeted therapies such as EGFR inhibitors in lung and colon cancer (Roberts et al., 2010; Bardelli and Siena, 2010). To address the challenge of selective targeting of cancer cells harboring oncogenic KRAS, many laboratory studies are focusing on signal transduction pathways downstream of KRAS, and several signaling molecules that are regulated by RAS, such as RAF, MEK, and PI3K, are being targeted by drugs in early clinical trials (Lim and Counter, 2005; Gupta et al., 2007; Engelman et al., 2008; Yu et al., 2008; Wee et al., 2009; Halilovic et al., 2010).

In addition to these efforts, which build on previous insights into the linear signaling pathways through which RAS promotes cellular viability and proliferation, several studies have used large-scale functional genomic screens to search for genes that are aberrantly required as a result of adaptation to a transforming KRAS mutation and might therefore represent new therapeutic targets (Barbie et al., 2009; Luo et al., 2009; Scholl et al., 2009; Wang et al., 2010; Vicent et al., 2010). Using high-throughput RNA interference (RNAi), we recently described that the expression of a functionally uncharacterized serine/threonine kinase, STK33, is required by human cancer cells that are dependent on mutant KRAS, but not untransformed cells or cancer cells with a different oncogenic lesion (Scholl et al., 2009). Although the role of STK33 in normal cellular physiology and in KRAS mutant cancer cells is not well understood, the enhanced STK33 dependence of KRAS mutant cells supports STK33 as an attractive target for therapy that could be pursued with drug discovery approaches. However, to inform this strategy, additional studies are necessary to better understand the functional link between mutant KRAS and STK33 and to elucidate the mechanism through which STK33 promotes cancer cell viability.

The primary goal of this study was to gain insight into the signaling pathways through which STK33 functions in human cancer cells. Using mass spectrometry–based proteomics, we observed that STK33 physically interacts with components of the HSP90 chaperone complex that is essential for the proper folding, stabilization, and activation of numerous proteins involved in cell survival and proliferation (Picard, 2002; Taipale et al., 2010), including oncoproteins that are mutated or overexpressed in certain cancer types (Gorre et al., 2002; George et al., 2004; Sawai et al., 2008; Cerchietti et al., 2009; Marubayashi et al., 2010). Genetic or pharmacologic inhibition of HSP90 in human cancer cell lines of various tissue origin induced proteasome-mediated degradation of STK33, resulting in apoptosis, both in vitro and in xenotransplant tumors, preferentially in cells harboring mutant KRAS. Furthermore, cells derived from KRAS mutant primary human colon carcinomas were significantly more sensitive to HSP90 inhibitor treatment. These findings identify STK33 as a new HSP90 client protein and provide mechanistic insight into the activity of HSP90 inhibitors in KRAS mutant cancer cells that has been noted before but remained unexplained until now (Wong et al., 2011; West et al., 2011; Sos et al., 2009). Furthermore, the data indicate that the requirement for STK33 may be exploited to target mutant KRAS-driven cancers, and suggest a therapeutic strategy that could be evaluated immediately because HSP90 inhibitors are currently undergoing clinical evaluation in patients with various malignancies. Finally, these results show that the optimal use of HSP90 inhibitors will depend on understanding the functional dependencies of specific cancers, and support KRAS mutation status as a marker for predicting responsiveness to these agents.

RESULTS

HSP90 binds to and stabilizes STK33 in human cancer cells

We used a mass spectrometry–based approach to identify STK33 protein interaction partners in human cancer cells. The breast cancer cell lines MDA-MB-231 (harboring a $KRAS^{G13D}$ mutation) and BT-20 (harboring WT KRAS) were stably transduced with a lentiviral vector encoding Flag-tagged STK33 or an empty control vector. Protein lysates of these cell lines were incubated with anti-Flag agarose, and isolated proteins were separated by PAGE (Fig. 1 a). Each lane was excised and divided into 10 equally sized pieces, and peptides were sequenced by microcapillary reverse-phase HPLC nanoelectrospray tandem mass spectrometry. The most highly enriched proteins in the STK33-expressing samples were two members of the HSP90 family of chaperones, HSP90AB1 (also known as HSP90B) and HSP90AA1 (also known as HSP90A). In addition, the HSP90 adaptor protein CDC37 was also significantly overrepresented in the STK33-expressing samples (Fig. 1 b). Coimmunoprecipitation (coIP) experiments with MDA-MB-231 cells stably expressing hemagglutinin (HA)-tagged STK33 confirmed the binding of STK33 to HSP90 and CDC37 (Fig. 1 c).

HSP90 is known to stabilize and activate multiple proteins (so-called "clients"; Picard, 2002; Taipale et al., 2010), several of which are mutated or overexpressed in human cancer (Gorre et al., 2002; George et al., 2004; Sawai et al., 2008; Cerchietti et al., 2009; Marubayashi et al., 2010). In some cases, HSP90 acts in a complex with CDC37, which specifically maintains the proper folding and function of protein kinases (Taipale et al., 2010). To investigate whether HSP90 is required for STK33 stability, we used lentiviral short hairpin RNA (shRNA) vectors to suppress HSP90A and HSP90B expression in a panel of lung and colon cancer cell lines that were dependent on mutant KRAS and STK33 as assessed by anchorage-independent growth in soft agar and tumor formation in immunocompromised mice (A549, HCT-116; Scholl et al., 2009), or that lacked mutant KRAS (NCI-H520, Caco-2). We determined STK33 protein levels by Western blot analysis. Knockdown of HSP90A and HSP90B depleted STK33 protein in all cell lines, irrespective of KRAS mutation status (Fig. 1 d). However, STK33 degradation was accompanied by induction of apoptosis, as indicated by increased PARP cleavage, in mutant KRAS- and STK33-dependent cell

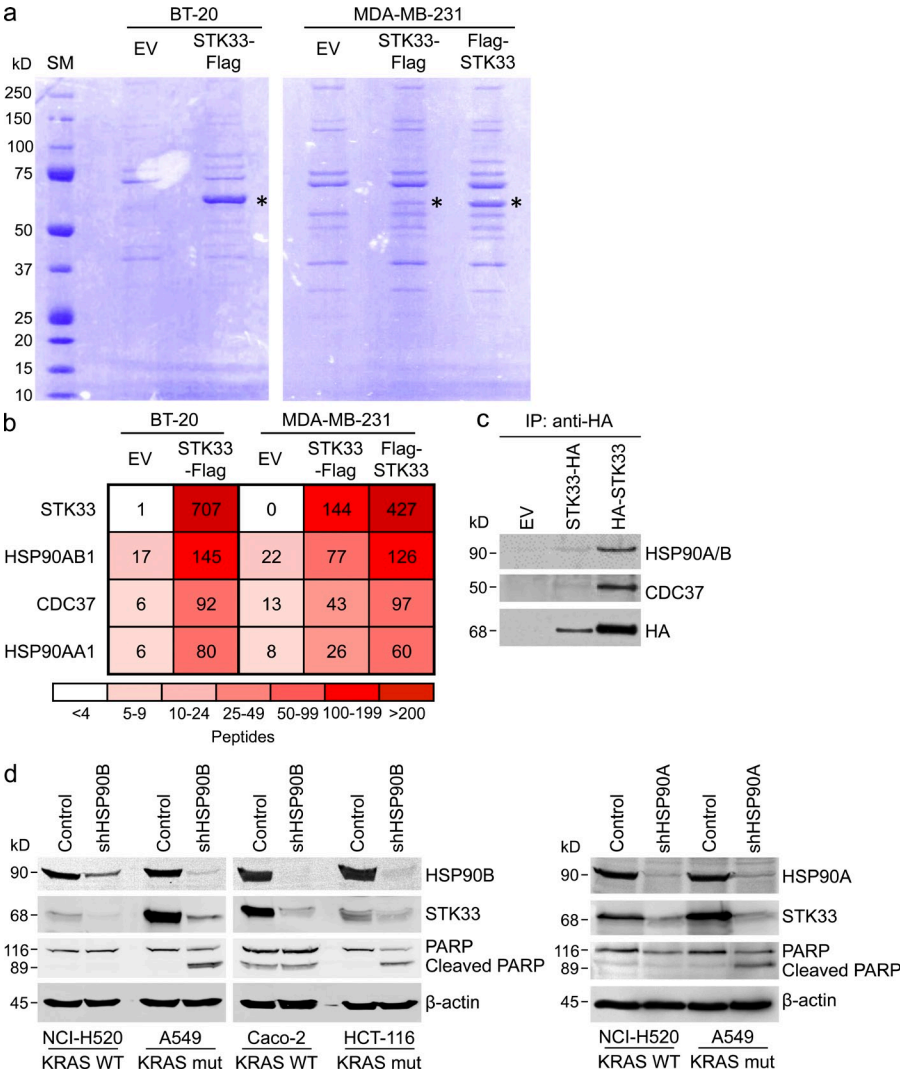

Figure 1. HSP90 associates with and stabilizes STK33. (a) Anti-Flag IPs were performed with KRAS WT BT-20 and KRAS mutant MDA-MB-231 breast cancer cell lines stably transduced with empty vector (EV), N-terminally Flag-tagged STK33 (Flag-STK33), or C-terminally Flag-tagged STK33 (STK33-Flag), and the resulting protein complexes were separated by PAGE and stained with Coomassie. Peptides isolated from each lane were analyzed by mass spectrometry. The STK33 band is indicated by an asterisk. SM, size marker. (b) Number of peptides representing proteins highly enriched in STK33-containing IPs. (c) Anti-HA IPs were performed with MDA-MB-231 cells stably transduced with empty vector (EV), N-terminally HA-tagged STK33 (HA-STK33), or C-terminally HA-tagged STK33 (STK33-HA), and immunoblots were probed with antibodies against HSP90A/B, CDC37, and HA. One of three independent experiments is shown. (d) Protein expression of HSP90A, HSP90B, STK33, and cleaved PARP in lung (NCI-H520, A549) and colon (Caco-2, HCT-116) carcinoma cells transduced with a nontargeting control shRNA or a shRNA-targeting HSP90A or HSP90B. One of two independent experiments is shown.

lines but not in cell lines harboring WT KRAS (Fig. 1 d). Together, these observations identified STK33 as a new HSP90 chaperone client and suggested STK33 depletion via HSP90 inhibition as a potential strategy to target mutant KRAS-dependent cancer cells.

Pharmacologic HSP90 inhibition degrades STK33 and induces apoptosis in mutant KRAS-dependent cancer cells

Because of its function in stabilizing various oncoproteins, HSP90 has emerged as a promising cancer drug target, and several ATP-competitive HSP90 inhibitors are currently under investigation in clinical trials (Taldone et al., 2008; Trepel et al., 2010). To address the possibility that the functional relationship between STK33 and HSP90 could be exploited therapeutically, we investigated whether pharmacologic HSP90 inhibition would have the same effect on STK33 stability as shRNA-mediated HSP90 knockdown, and whether depletion of STK33 through HSP90 inhibition would induce apoptosis preferentially in cancer cells that rely on mutant KRAS for their survival.

We treated 12 human cancer cell lines (KRAS mutant, $n = 6$; KRAS WT, $n = 6$), representing four different cancer types (lung cancer, colon cancer, breast cancer, and acute myeloid leukemia [AML]), with increasing concentrations of two different compounds; the benzoquinone ansamycin 17-AAG, the first HSP90 inhibitor that entered clinical trials (Kim et al., 2009); and PU-H71, an optimized, water-soluble member of the purine class of HSP90 inhibitors (Taldone and Chiosis, 2009). We observed that both inhibitors caused dose-dependent degradation of STK33 in all cell lines, regardless of tissue origin or KRAS mutation status (Fig. 2 a and not depicted). Analysis of PARP cleavage showed that all six cell lines with mutant KRAS underwent apoptosis in response to HSP90 inhibitor treatment, whereas the KRAS WT cell lines were unaffected. Administration of 17-AAG or PU-H71 also led to increased cleavage and activity of caspase 9 in KRAS mutant, but not KRAS WT cell lines (Fig. 2, a and b), consistent with previous data showing that apoptosis induced by STK33 suppression in mutant KRAS-dependent cells is mediated via the mitochondrial pathway (Scholl et al., 2009). Monitoring of cell viability in the presence of low PU-H71 concentrations also demonstrated the higher sensitivity of mutant KRAS-dependent cell lines to this compound (Fig. 2 c). These findings indicated that, because of their ability to efficiently degrade STK33, HSP90 inhibitors may represent an approach to targeting human cancers

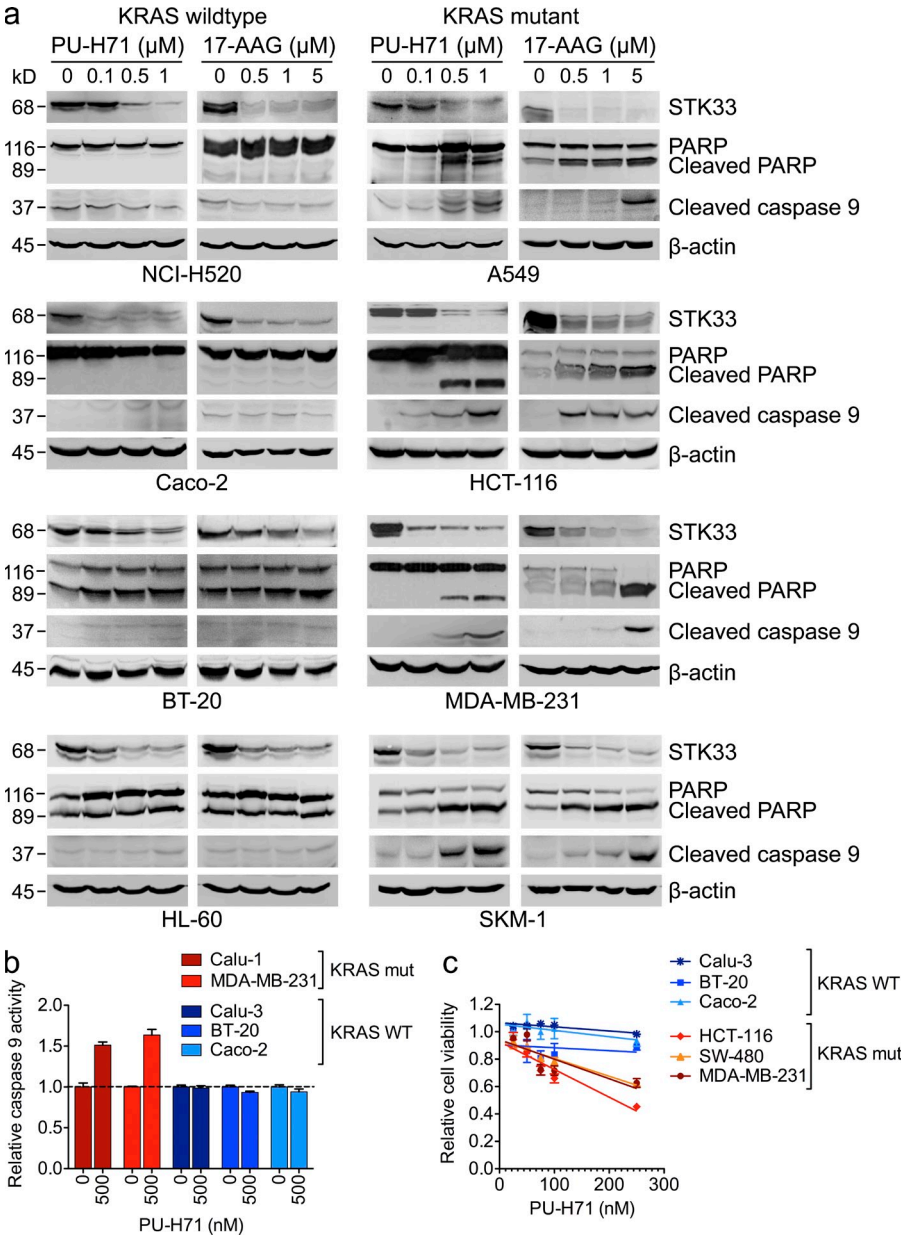

Figure 2. Pharmacologic inhibition of HSP90 depletes STK33 and preferentially induces apoptosis in mutant KRAS-dependent cancer cells. (a) Immunoblots of lung cancer (NCI-H520, A549), colon cancer (Caco-2, HCT-116), breast cancer (BT-20, MDA-MB-231), and AML (HL-60, SKM-1) cell lines incubated with increasing concentrations of PU-H71 or 17-AAG for 24 h. (b) Caspase 9 activity in KRAS mutant (mut) and KRAS WT cancer cell lines incubated with 0.5 μM PU-H71 for 24 h. Experiments were done in triplicate. Error bars represent mean ± SEM. One of two independent experiments is shown. (c) Viability and proliferation of mutant KRAS-dependent (mut) and KRAS WT cancer cell lines incubated with low PU-H71 concentrations for 48 h. Experiments were done in triplicate. Error bars represent mean ± SEM. One of two independent experiments is shown.

associated with mutant KRAS essentiality, and confirmed previous observations that suppression of STK33 kills mutant KRAS-dependent cancer cells of various tissue origin (Scholl et al., 2009).

Degradation of STK33 is essential for enhanced killing of mutant KRAS-dependent cancer cells by HSP90 inhibitors

HSP90 is involved in stabilizing multiple proteins that promote cancer cell survival, including known RAS effectors such as components of the PI3K-AKT and MAPK signaling pathways (Picard, 2002; Taipale et al., 2010). We therefore sought additional evidence that the induction of apoptosis in mutant KRAS-dependent cancer cells upon HSP90 inhibition can be attributed to depletion of STK33.

We first performed time course experiments to determine whether down-modulation of STK33 preceded the induction of apoptosis. We treated mutant KRAS- and STK33-dependent MDA-MB-231 and A549 cells with 5 μM 17-AAG or 1 μM PU-H71 for 4, 8, 12, 16, 20, and 24 h and observed that STK33 levels began to decrease at 4 h, with maximum depletion occurring after 12 h. STK33 degradation was followed by PARP cleavage after 12–16 h, consistent with causality between reduction in STK33 protein expression and apoptosis induction, rather than an unspecific change associated with cell death (Fig. 3 a and not depicted). In contrast, cellular KRAS levels were not reduced by treatment with PU-H71 (unpublished data), confirming previous observations that KRAS is not an HSP90 client (Sos et al., 2009).

Second, we investigated whether forced expression of STK33 protected mutant KRAS-dependent cells from the apoptotic effects of HSP90 inhibition, as this would confirm STK33 as a protein whose depletion mediates the sensitivity of mutant KRAS-driven cells to HSP90 inhibition. We treated MDA-MB-231, A549, and Calu-1 cells overexpressing STK33 with increasing concentrations of 17-AAG or PU-H71 and determined the abundance of STK33 and cleaved PARP by Western blot analysis. As expected, exogenous STK33 was also subject to degradation; however, the higher remaining STK33 levels partially rescued cell viability after HSP90 inhibitor treatment in a dose-dependent manner (Fig. 3 b and not depicted). Overexpression of STK33 also reduced caspase 9 activity and led to a shift of the dose–response curve in mutant KRAS-dependent

cells after treatment with PU-H71 (Fig. 3 c and not depicted). In contrast, exogenous STK33 did not prevent apoptosis in MDA-MB-453 breast cancer cells and MOLM-14 AML cells that are known to be highly dependent on different HSP90 clients (ERBB2 [also known as HER2] and FLT3, respectively), indicating that the partial rescue observed in KRAS mutant cells was not an unspecific effect caused by supraphysiological expression of STK33 (Fig. 3 d).

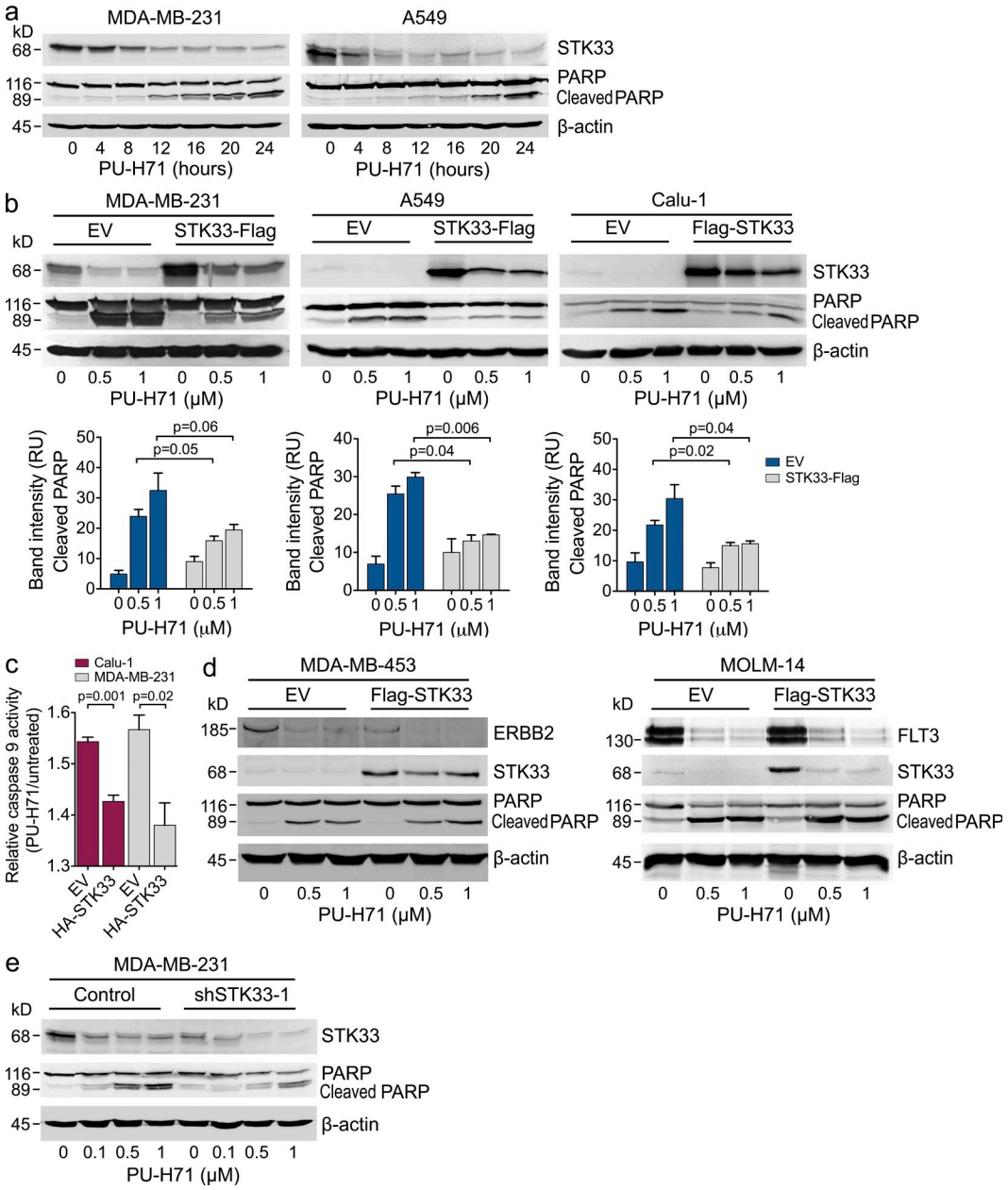

Figure 3. Causal relationship between degradation of STK33 and killing of mutant KRAS-dependent cancer cells by HSP90 inhibitors. (a) Immunoblots of mutant KRAS-dependent breast cancer (MDA-MB-231) and lung cancer (A549) cell lines incubated with 1 μM PU-H71 for the indicated times. (b) Immunoblot of MDA-MB-231, A549, and Calu-1 cells stably transduced with empty vector (EV) or STK33 and incubated with different concentrations of PU-H71 for 24 h. Cleaved PARP bands were quantified by densitometric analysis using the ImageJ program. Results of two to three independent experiments are shown. RU, relative unit. (c) Caspase 9 activity in KRAS mutant breast cancer (MDA-MB-231) and lung cancer (Calu-1) cell lines transduced with empty vector (EV) or STK33 and incubated with 0.5 μM PU-H71 for 24 h. Experiments were done in triplicate. Error bars represent mean ± SEM. (d) Immunoblot of KRAS WT MDA-MB-453 breast cancer (ERBB2-amplified) and MOLM-14 AML (FLT3-mutated) cells stably transduced with empty vector (EV) or STK33 and incubated with different concentrations of PU-H71 for 24 h. (e) Immunoblot of MDA-MB-231 cells that evaded apoptosis induced by shRNA-mediated STK33 knockdown after incubation with increasing concentrations of PU-H71 for 24 h. All results were confirmed in at least one additional independent experiment.

Third, we cultured MDA-MB-231 cells stably expressing a shRNA targeting STK33 over a period of 3 wk and isolated the cells that evaded apoptosis despite sufficient STK33 knockdown. In agreement with the hypothesis that these "escaper" cells also had diminished sensitivity to STK33 depletion via HSP90 inhibition, treatment with 17-AAG or PU-H71 resulted in reduced PARP cleavage compared with cells transduced with a nontargeting control shRNA (Fig. 3 e and not depicted).

Finally, we examined whether the genotype-selective effect of HSP90 inhibitor treatment might be caused by depletion of other proteins involved in KRAS-mediated oncogenesis that have been reported to be HSP90 clients. Specifically, we focused on the serine/threonine kinases RAF1 and AKT1 that are immediate downstream effectors of KRAS. Treatment of MDA-MB-231 cells with 1 µM PU-H71 over 24 h resulted in efficient RAF1 and AKT1 depletion in a time-dependent manner comparable to STK33 (Fig. 4 a). This suggested that depletion of RAF1 or AKT1 might contribute to apoptosis induction in KRAS mutant cells after HSP90 inhibition. To investigate this possibility, we evaluated RAF1 and AKT1 dependence in three KRAS mutant cancer cell lines using shRNA-mediated RNAi. Suppression of RAF1 and AKT1 increased apoptosis in HCT-116 colon cancer cells, but not in A549 lung cancer cells and MDA-MB-231 breast cancer cells, arguing against RAF1 and AKT1 as the HSP90 clients responsible for the genotype-selective effect of HSP90 inhibitors across different tissues (Fig. 4, b and c). Consistent with this conclusion, overexpression of RAF1 and AKT1 in these cell lines did not rescue cell viability after PU-H71 treatment (Fig. 4 d).

Together, these data supported the concept that degradation of STK33 is required for killing of KRAS mutant cancer cells of diverse tissue origin by 17-AAG or PU-H71, and indicated that the degree of dependence on STK33 dictates the sensitivity of human cancer cells to HSP90 inhibition. Depletion of other clients, such as RAF1 and AKT1, probably contributes to the apoptotic effect of HSP90 inhibitors in cells that rely on the expression of these proteins.

HSP90 inhibition induces ubiquitination and proteasomal degradation of STK33

We next evaluated the mechanism of STK33 depletion caused by HSP90 inhibitor treatment. To investigate whether STK33 is degraded via the lysosomal pathway, we incubated KRAS mutant A549 lung cancer cells with the lysosome inhibitor NH_4Cl followed by PU-H71 treatment, and determined the abundance of STK33 protein in the detergent-soluble and

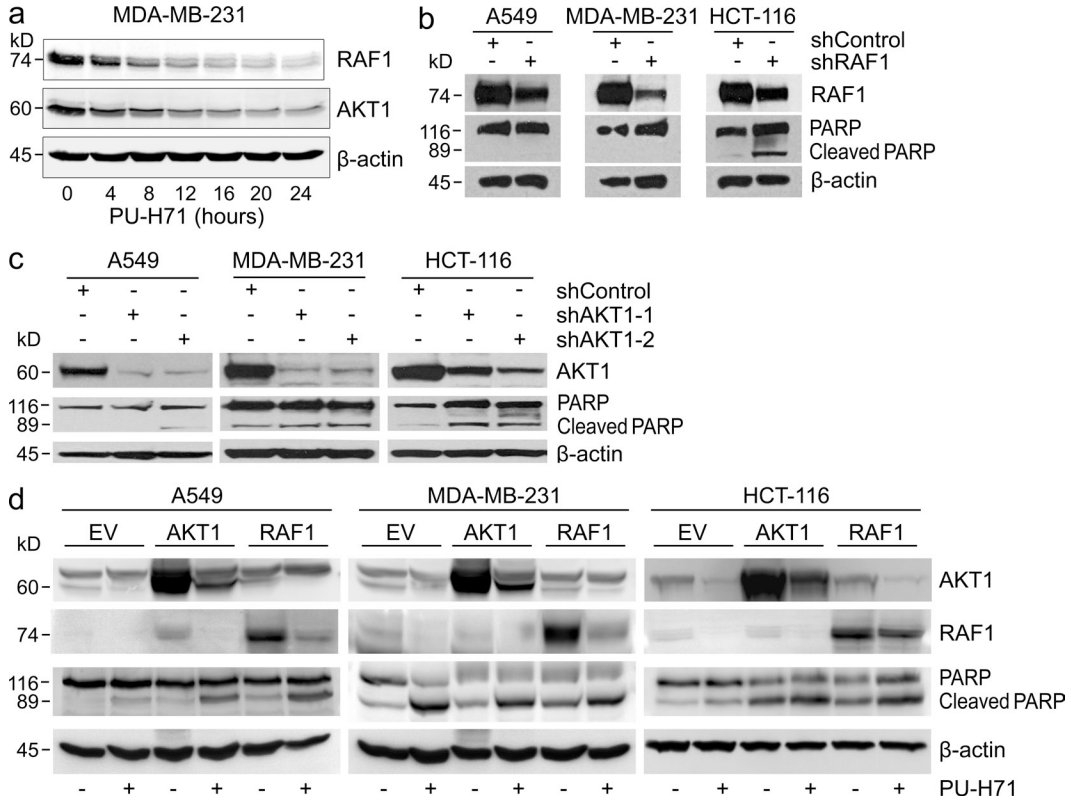

Figure 4. Relationship between degradation of AKT1 or RAF1 and killing of mutant KRAS-dependent cancer cells by HSP90 inhibitors. (a) Immunoblots of MDA-MB-231 cells incubated with 1 µM PU-H71 for the indicated times showing depletion of AKT1 and RAF1. (b and c) PARP cleavage in mutant KRAS-dependent lung cancer (A549), breast cancer (MDA-MB-231), and colon cancer (HCT-116) cell lines transduced with shRNAs targeting AKT1 (c) and RAF1 (b), respectively, or a nontargeting control shRNA. (d) Immunoblots of A549, MDA-MB-231, and HCT-116 cells stably transduced with empty vector (EV), AKT1, or RAF1 and incubated with 1 µM PU-H71 for 24 h. All results were confirmed in at least one additional independent experiment.

insoluble fractions by Western blot analysis. Pretreatment with NH_4Cl did not increase STK33 protein levels compared with incubation with PU-H71 alone, indicating that STK33 is not degraded via the lysosomal pathway (Fig. 5 a). In contrast, treatment of A549 cells with two proteasome inhibitors, MG-132 and bortezomib, followed by incubation with PU-H71 rescued STK33 protein levels and resulted in redistribution of STK33 to the detergent-insoluble fraction; this result was confirmed in MDA-MB-231 and HCT-116 cells (Fig. 5 b and not depicted). Consistent with its degradation via the proteasomal pathway, STK33 was extensively ubiquitinated in 293T cells after treatment with PU-H71 in combination with MG-132, resulting in a molecular weight of more than 250 kD (Fig. 5 c).

To search for proteins that might regulate STK33 stability, we interrogated the list of candidate STK33 interaction partners identified in the mass spectrometry experiment shown in Fig. 1 a. Among the proteins enriched in STK33-containing IPs were BAG2, a BAG domain-containing protein that inhibits the degradation of chaperone-bound cytoplasmic proteins via the ubiquitin/proteasome system (Dai et al., 2005); USP5 and USP15, two ubiquitin-specific peptidases; and HERC2, an E3 ubiquitin ligase (Fig. 5 d). To evaluate whether BAG2 is involved in the control of STK33 stability, we transduced MDA-MB-231 and A459 cells with a lentiviral vector encoding BAG2 and determined STK33 protein abundance after treatment with PU-H71. Consistent with the hypothesis that BAG2 inhibits STK33 degradation, BAG2 overexpression rescued STK33 protein levels in the presence of PU-H71 in both

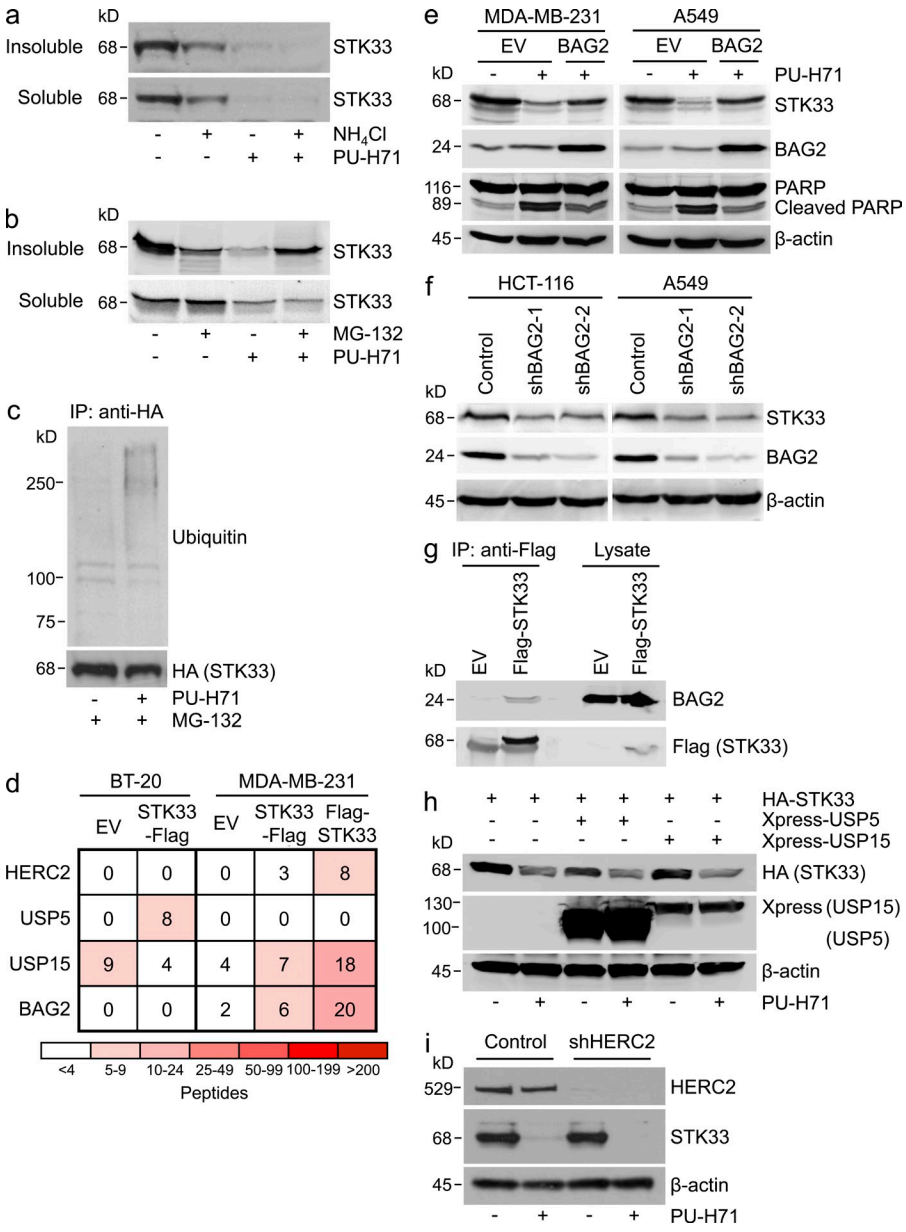

Figure 5. PU-H71 induces ubiquitination and proteasomal degradation of STK33. (a) Immunoblot of A549 cells treated with 20 mM NH_4Cl for 2 h, followed by incubation with 0.5 µM PU-H71 for 16 h. One of two independent experiments is shown. (b) Immunoblot of A549 cells treated with 10 µM MG-132 for 2 h, followed by incubation with 0.5 µM PU-H71 for 16 h. (c) IP of HA-tagged STK33 from 293T cells treated with or without 1 µM PU-H71 for 7 h and 10 µM MG-132 for the final 3 h. Ubiquitinated STK33 appears as a smear with high molecular weight. One of three independent experiments is shown. (d) Anti-Flag IPs were performed with KRAS WT BT-20 and mutant KRAS-dependent MDA-MB-231 cells stably transduced with empty vector (EV), N-terminally Flag-tagged STK33 (Flag-STK33), or C-terminally Flag-tagged STK33 (STK33-Flag), and the resulting protein complexes were analyzed by mass spectrometry. The enrichment of peptides representing proteins involved in the ubiquitin/proteasome system is shown. (e) Immunoblot of MDA-MB-231 and A549 cells transduced with empty vector (EV) or BAG2 and treated with 0.5 µM PU-H71 for 24 h. (f) Immunoblot of HCT-116 and A549 cells transduced with a nontargeting control shRNA or shRNAs targeting BAG2. (g) Anti-Flag IPs were performed with MDA-MB-231 cells stably transduced with empty vector (EV) or Flag-tagged STK33, and immunoblots were probed with antibodies against BAG2 and Flag. One of two independent experiments is shown. (h) Immunoblot of 293T cells transfected with HA-tagged STK33 or Xpress-tagged USP15 and USP5, respectively, and treated with or without 0.5 µM PU-H71 for 24 h. One of two independent experiments is shown. (i) MDA-MB-231 cells were transfected with a nontargeting control shRNA or a shRNA targeting HERC2. After 3 d, cells were incubated with 1 µM PU-H71 for 18 h, as indicated. Protein levels were analyzed by Western blotting using the indicated antibodies. One of two independent experiments is shown.

cell lines, and this was associated with decreased apoptosis, as indicated by reduced PARP cleavage (Fig. 5 e). Conversely, shRNA knockdown of BAG2 in HCT-116 and A549 cells decreased STK33 expression (Fig. 5 f). Binding of BAG2 to STK33 was confirmed in coIP experiments with MDA-MB-231 cells stably expressing Flag-tagged STK33 (Fig. 5 g). To examine whether USP5 and USP15 can deubiquitinate STK33, we analyzed 293T cells co-transfected with HA-tagged STK33 and either USP5 or USP15. Neither USP5 nor USP15 overexpression protected STK33 from HSP90 inhibitor-induced degradation, indicating that other ubiquitin-specific peptidases are involved in regulating STK33 stability (Fig. 5 h). To investigate whether HERC2 attaches ubiquitin to STK33 after HSP90 inhibition, we determined STK33 protein levels in the context of HERC2 knockdown in MDA-MB-231 cells after treatment with PU-H71. Depletion of HERC2 did not enhance STK33 stability, arguing against HERC2 as an STK33-specific ubiquitin ligase (Fig. 5 i). Together, these findings demonstrated that degradation of STK33 upon HSP90 inhibition occurs via the proteasomal pathway and is negatively regulated by BAG2.

HSP90 inhibition impairs growth of mutant KRAS-dependent tumors in vivo in an STK33-dependent manner

To verify the genotype-dependent apoptotic effect of HSP90 inhibitors in vivo, we first performed xenotransplantation experiments using a chicken chorioallantoic membrane (CAM) assay that mitigates pharmacokinetic liabilities of certain HSP90 inhibitors in rodent xenograft models. Mutant KRAS-dependent HCT-116 and KRAS WT Caco-2 colon cancer cells were deposited on the surface of chicken CAM 8 d after fertilization, and tumor formation was observed after 24 h. 17-AAG (5 µM) and PU-H71 (1 µM) were administered 24 and 48 h after implantation, and xenograft tumors were measured and analyzed by immunohistochemistry (IHC) after 72 h. Treatment of HCT-116 cells with either inhibitor resulted in a significant decrease in tumor size, whereas Caco-2 cells were unaffected (Fig. 6 a). IHC analysis showed that STK33 was efficiently degraded in all tumors after incubation with HSP90 inhibitors (Fig. 6 b). However, enhanced apoptosis, as assessed by terminal deoxynucleotidyl transferase dUTP nick end labeling (TUNEL), was only observed in KRAS mutant HCT-116 cells, but not in KRAS WT Caco-2 cells (Fig. 6 c). The effects of HSP90 inhibition on

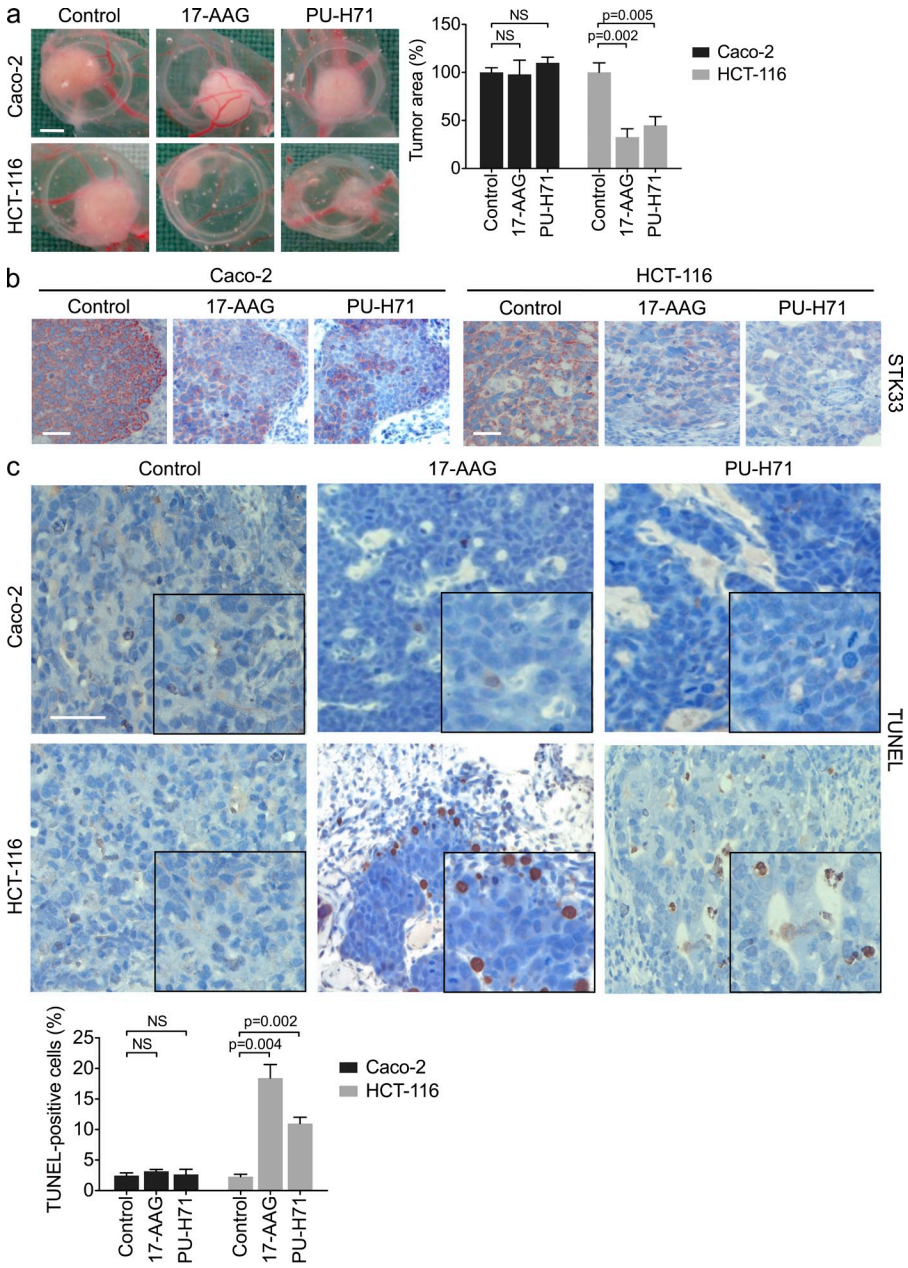

Figure 6. HSP90 inhibition impairs the growth of mutant KRAS-dependent colon tumors on chicken CAM. (a) Tumor formation on chicken CAM of KRAS WT (Caco-2) and mutant KRAS-dependent (HCT-116) colon cancer cell lines treated with 5 µM 17-AAG or 1 µM PU-H71 or vehicle for 48 h. Representative photographs of tumors (cells were deposited within a 5-mm silicon ring to allow drug administration) and tumor areas (error bars represent mean ± SEM of four to six tumors) are shown. Bar, 1.5 mm. (b and c) IHC analysis of CAM tumors shown in a. STK33 protein expression (b) and TUNEL staining (c) of Caco-2 and HCT-116 tumors. Representative photographs of tissue sections and the proportion of TUNEL-positive cells (error bars represent mean ± SEM of four microscopic fields with 600 cells) are shown. NS, not significant. Insets in c show details of the corresponding photographs. Bar: 125 µm; inset, 25 µm.

tumor growth and cell viability in the context of mutant KRAS dependence could be recapitulated in MDA-MB-231 breast cancer cells (Fig. 7, a and b). The cytotoxicity of 17-AAG and PU-H71 was reversed by exogenous overexpression of STK33, as indicated by restored tumor formation and diminished apoptosis, again supporting a causal relationship between STK33 depletion and killing of mutant KRAS-dependent cancer cells through HSP90 inhibition (Fig. 7, a and b). The specificity of the STK33 antibody used for IHC was confirmed by staining of xenograft tumors derived from cancer cell lines that were stably transduced with three different shRNAs targeting STK33 and grown on CAM or in nude mice (unpublished data).

Based on these observations in the chicken CAM xenograft system, we sought confirmation in immunodeficient mice. We first assessed the kinetics of STK33 degradation in vivo by transplantation of HCT-116 cells s.c. into nude mice and, after tumor formation, we injected either 75 mg per kg body weight PU-H71 or PBS i.p. Mice were sacrificed 12, 24, 48, and 72 h later, and STK33 protein levels in tumors were determined by Western blot analysis. STK33 degradation was evident 12 h after treatment and was sustained beyond 72 h (Fig. 8 a). To evaluate the effect of PU-H71 treatment on tumor growth, we injected mutant KRAS-dependent (SW-480, HCT-116) and KRAS WT (Caco-2, Colo-320HSR) colon cancer cell lines s.c. into both flanks of nude mice. After the formation of tumors, mice received either 75 mg per kg body weight PU-H71 or vehicle (PBS) i.p. 3 times per wk. Tumor growth was monitored, and mice were sacrificed when tumors reached the maximum size permitted by the institutionally approved protocol (Colo-320HSR), or after 3 wk (SW-480, HCT-116, Caco-2). Consistent with the in vitro and CAM assays, growth of KRAS mutant tumors was substantially inhibited by PU-H71, whereas KRAS WT tumors were unaffected (Fig. 8 b). Furthermore, apoptosis, as assessed by TUNEL, was selectively increased in KRAS mutant tumors (Fig. 8 c). Degradation of STK33 protein in tumors was verified by Western blot analysis (Fig. 8 d). These data demonstrated that HSP90 inhibition efficiently depletes STK33 in vivo and impairs tumor formation of KRAS mutant cancer cells in an STK33-dependent manner.

Effects of HSP90 inhibition on primary human colon tumor-initiating cells

To evaluate whether the findings in cell lines could be extrapolated to primary human cancer cells, we generated sphere cultures that allow the enrichment and expansion of cells with tumor-initiating properties from five surgically resected colon carcinomas. DNA sequence analysis identified a *KRAS* mutation in three of the five samples (Fig. 9 a). To examine the response to HSP90 inhibition, single cells were seeded in 96-well plates and incubated with 0.5 µM PU-H71 for 48 h. Sphere formation of KRAS mutant cells was abrogated by PU-H71, whereas KRAS WT cells showed residual sphere-forming capacity (Fig. 9 b). Furthermore, PU-H71 had a significantly stronger inhibitory

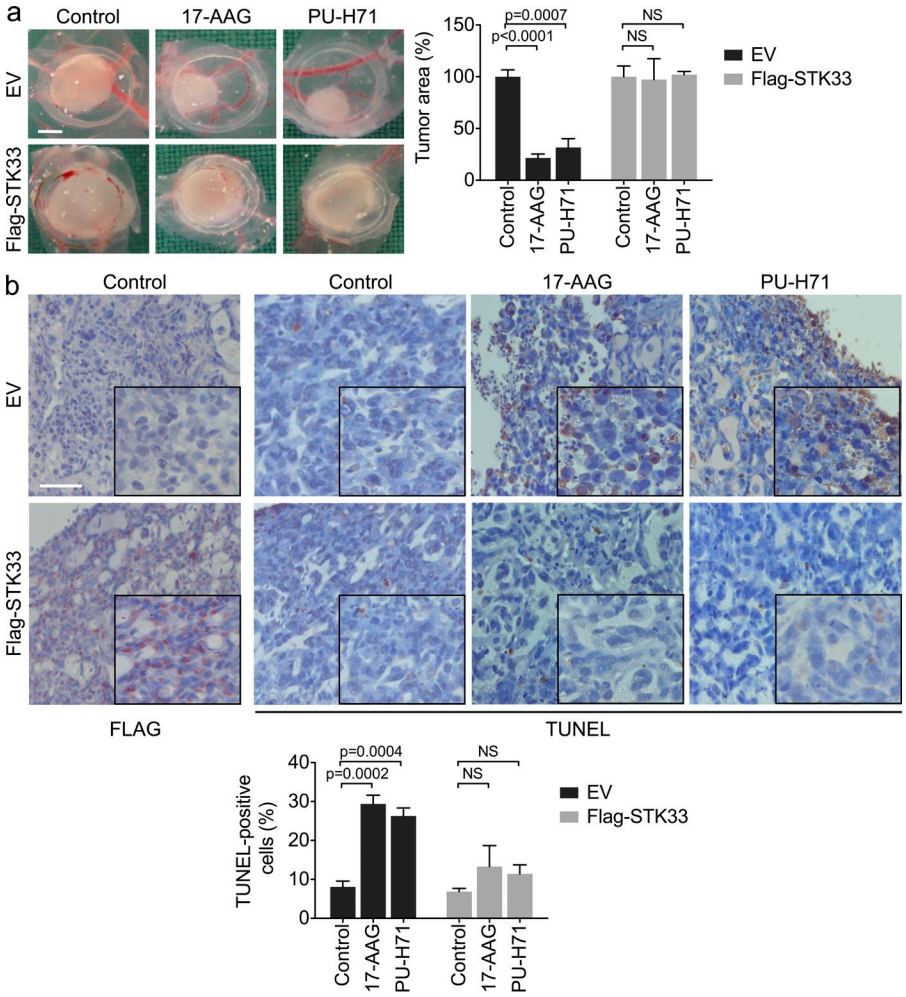

Figure 7. STK33 overexpression restores the growth of mutant KRAS-dependent breast tumors treated with HSP90 inhibitors. (a) Tumor formation on chicken CAM of mutant KRAS-dependent MDA-MB-231 breast cancer cells stably transduced with Flag-tagged STK33 or empty vector (EV) and treated with 5 µM 17-AAG or 1 µM PU-H71 for 48 h. Representative photographs of tumors and tumor areas (error bars represent mean ± SEM of four to six tumors) are shown. NS, not significant. Bar, 1.5 mm. (b) IHC analysis of CAM tumors shown in a. Representative photographs of tissue sections and the proportion of TUNEL-positive cells (error bars represent mean ± SEM of four microscopic fields with 600 cells) are shown. EV, empty vector. Insets show details of the corresponding photographs. Bar: 125 µm; inset, 25 µm.

effect on cell viability and proliferation in KRAS mutant versus KRAS WT cultures (Fig. 9, c and d). Together, these results indicated that HSP90 inhibitors target KRAS mutant primary human colon cancer cells with tumor-initiating capacity, further supporting the idea that HSP90 inhibitors could be effective in the treatment of KRAS mutant cancers.

DISCUSSION

Inhibition of constitutively active KRAS has long been pursued as a potential strategy for the treatment of cancer. However, attempts to target mutant KRAS directly have not met with success (Downward, 2003; Malumbres and Barbacid, 2003; Roberts and Der, 2007). To overcome this challenge, several studies have identified co-dependencies that KRAS mutant cancer cells have on interacting nononcogenes, which encode a wide range of proteins, such as kinases, transcriptional regulators, and adhesion molecules (Singh et al., 2009; Scholl et al., 2009; Luo et al., 2009; Barbie et al., 2009; Puyol et al., 2010; Wang et al., 2010; Vicent et al., 2010). Although these molecules represent promising therapeutic targets, in principle, no specific inhibitors exist for most of them. In addition, the mechanistic underpinnings of the requirement for certain nononcogenes in KRAS mutant cancer cells are unknown, further complicating efforts to develop small molecules that target such dependencies.

To work toward genotype-informed treatment of cancers driven by mutant KRAS, we focused on STK33, a serine/threonine kinase of unknown function that is selectively required by mutant KRAS-dependent human cancer cell lines (Scholl et al., 2009). Using a quantitative protein interaction screen, we found that STK33 is a novel client of the HSP90 chaperone complex. Pharmacologic inhibition of HSP90 with

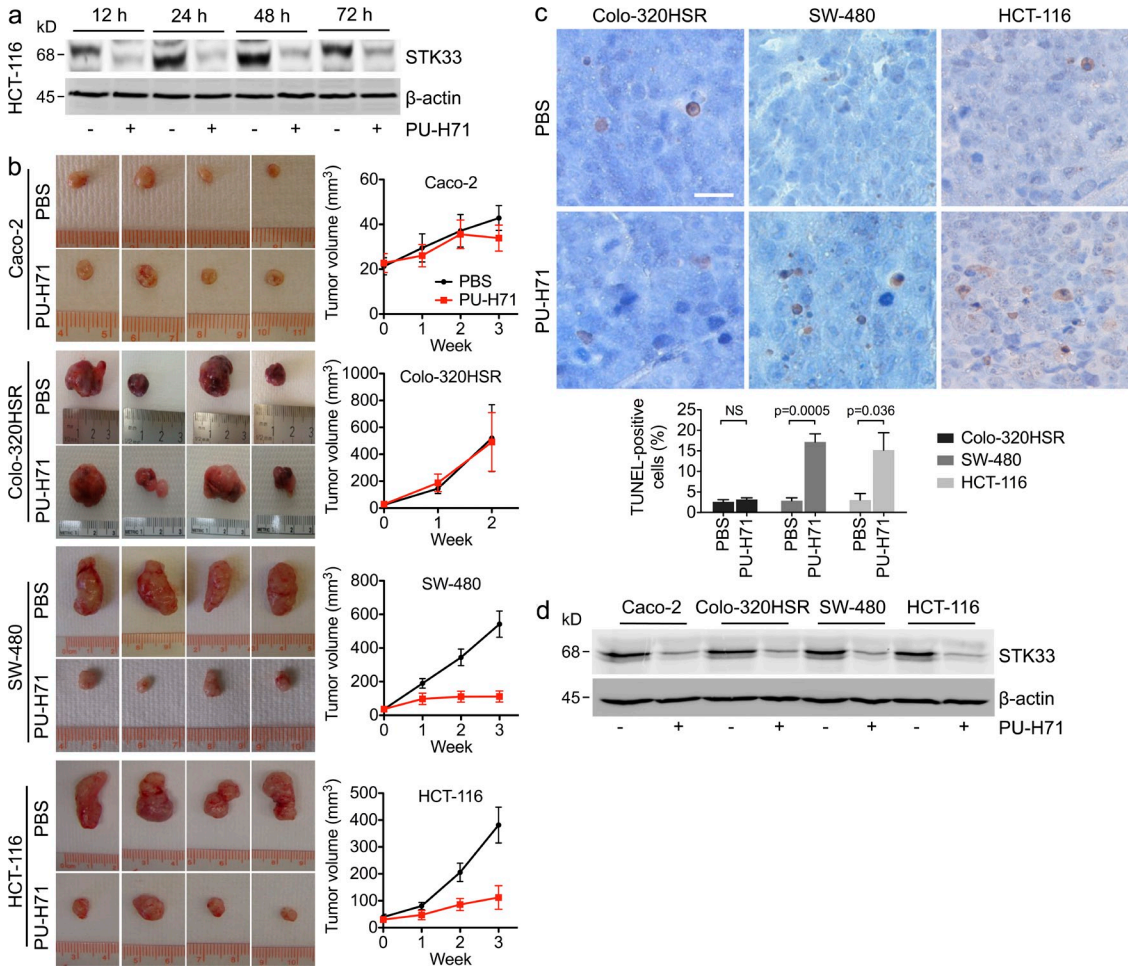

Figure 8. HSP90 inhibition impairs the growth of mutant KRAS–dependent tumors in nude mice. (a) Immunoblot of HCT-116 tumors. After tumor formation, mice were injected once with 75 mg per kg body weight PU-H71 or PBS, and tumors were harvested after the indicated times. One mouse per condition and time point was analyzed. (b) Effects of PU-H71 on tumor formation of mutant KRAS-dependent (SW-480, HCT-116) and KRAS WT (Caco-2, Colo-320HSR) colon cancer cell lines in nude mice. Photographs of representative tumors and tumor volumes (error bars represent mean ± SEM of 7–14 tumors from 4–7 mice) are shown. (c) IHC analysis of tumors shown in b. Representative photographs of tissue sections and the proportion of TUNEL-positive cells (error bars represent mean ± SEM of four microscopic fields with 600–800 cells) are shown. NS, not significant. Bar, 125 µm. (d) Immunoblot of tumors shown in b demonstrating STK33 expression in treated mice. Tumors were harvested 24 h after the last injection.

a

ID	Age/ Sex	Tumor site	Tumor stage (UICC)	Tumor differentiation	KRAS status
SC-01	64/m	Liver metastasis	IV	Moderate	Mutant (G12V)
SC-02	54/m	Liver metastasis	IV	Moderate	Wildtype
SC-03	53/m	Right colon	IV	Poor	Wildtype
SC-04	68/m	Lung metastasis	IV	Moderate	Mutant (G12D)
SC-05	49/f	Liver metastasis	IV	Moderate	Mutant (G12A)

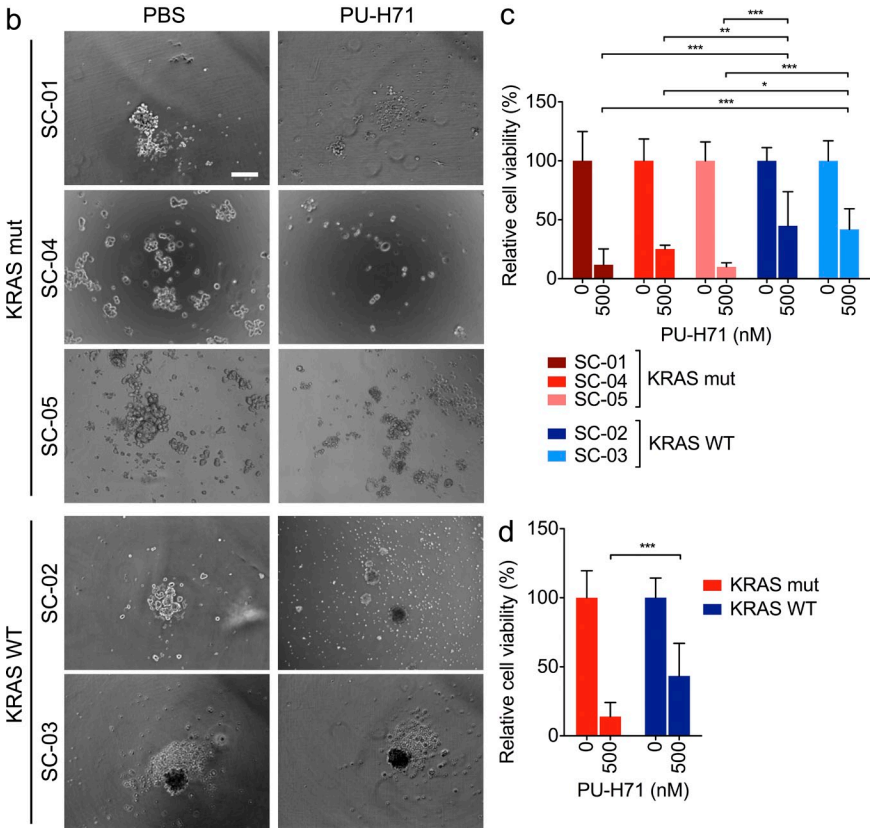

Figure 9. HSP90 inhibition impairs the survival of primary KRAS mutant colon tumor-initiating cells. (a) Characteristics of primary human colon cancer samples used for the generation of sphere cultures. (b) Photographs of colon cancer sphere cultures treated with 0.5 µM PU-H71 or PBS for 48 h. Bar, 200 µm. (c) Viability and proliferation of colon cancer sphere cultures incubated with 0.5 µM PU-H71 for 48 h. 6–12 independent experiments were done. Error bars represent mean ± SD. (d) Cumulative analysis of the response to PU-H71 of the different patient-derived sphere cultures according to KRAS status. *, $P < 0.05$; **, $P < 0.01$; ***, $P < 0.0001$.

structurally divergent small molecules resulted in destabilization and proteasomal degradation of STK33, regardless of cell type and KRAS mutation status. On the functional level, however, HSP90 inhibitors were preferentially toxic to mutant KRAS-driven cells of various tissue origin, both in vitro and in vivo, supporting the view that STK33 represents a relevant target in this particular context. A correlation between mutant KRAS and sensitivity to treatment with HSP90 inhibitors of the ansamycin family was recently observed in human lung cancer cell lines and a mouse model of lung adenocarcinoma (Sos et al., 2009), as well as in human colon cancer cell lines (West et al., 2011). Furthermore, clinical activity of the second-generation HSP90 inhibitor ganetespib was noted in patients with KRAS mutant non–small cell lung cancer (Wong et al., 2011). Our data now provide a molecular explanation for this association and demonstrate that it can be extrapolated to other cancers with KRAS mutations.

Abundant preclinical evidence indicates that HSP90 inhibitors are potent anticancer agents because of their capacity to compromise the stability of key oncogenic proteins, such as BCR-ABL1, EGFR, ERBB2, FLT3, JAK2, and BCL6, which drive malignant transformation through mutational activation or overexpression (Mimnaugh et al., 1996; Gorre et al., 2002; George et al., 2004; Sawai et al., 2008; Cerchietti et al., 2009; Marubayashi et al., 2010). In this context, the cytotoxic effect of HSP90 inhibition can be attributed to oncogene addiction, the dependence of a tumor on a particular oncogene that is altered in that tumor. The data reported here illustrate that in cancer cells, HSP90 is also important for maintaining the function of gene products that lack structural abnormalities or deregulated expression, but nevertheless exhibit essentiality in specific contexts, and thereby expand the repertoire of indications for HSP90 inhibitors to secondary, nononcogene dependencies. This might be particularly relevant in the context of intractable oncoproteins that cannot be inhibited directly and are not HSP90 clients, such as mutant KRAS.

Given that HSP90 stabilizes diverse regulators of cell viability and proliferation (Taipale et al., 2010), it often remains elusive whether cell killing upon HSP90 inhibition is mediated by depletion of a single client or simultaneous degradation of multiple proteins required for the transformed phenotype. In addition, it has been postulated that HSP90 inhibitors may act through a more general effect on protein homeostasis. Our findings indicate that the exquisite sensitivity of mutant KRAS-dependent cancer cells to these agents is primarily related to

depletion of STK33. First, the degradation of STK33 induced by HSP90 inhibitor treatment preceded apoptosis and thus did not represent an unspecific change associated with cell death. Second, forced expression of STK33-rescued cell viability after HSP90 inhibitor treatment in KRAS mutant cells, but not in KRAS WT cancer cells that are dependent on a different HSP90 client. Third, KRAS mutant cancer cells that had escaped the apoptotic effect of RNAi-mediated STK33 knockdown were partially resistant to 17-AAG and PU-H71. In contrast to these observations, depletion of RAF1 and AKT1, which are established KRAS effectors that are also known to be HSP90 clients, resulted in apoptosis only in a subset of KRAS mutant cell lines. Thus, although it is clear that various HSP90 substrates contribute to the anticancer effects of HSP90 inhibitors in different contexts, STK33 dependence emerges as an important determinant of the response of KRAS mutant cells to these agents. These data not only provide mechanistic insight into the activity of HSP90 inhibitors in KRAS mutant tumors, but also provide additional compelling evidence for a preferential requirement for STK33 in mutant KRAS-dependent cancer cells. Like shRNA-mediated knockdown, HSP90 inhibitors target mutant KRAS-driven cancer cells through depletion of the entire STK33 protein. This property may be of particular relevance in view of recent observations that selective inhibition of STK33 enzymatic activity does not kill certain KRAS mutant cancer cell lines (Babij et al., 2011; Luo et al., 2012), indicating that nonkinase activities of STK33 may be responsible for its observed essentiality in RNAi-based studies, an important disparity that has also been reported for Aurora B and PI3 kinases (Weiss et al., 2007).

More generally, our results emphasize the need for predictive markers of benefit from HSP90 inhibitors. Early clinical trials have suggested that HSP90 inhibitors are not sufficiently effective in many cancers (Barginear et al., 2008; Mahalingam et al., 2009; Trepel et al., 2010). However, although there are several established pharmacodynamic biomarkers of HSP90 modulation (Banerji et al., 2005; Zhang et al., 2006; Maloney et al., 2007), few studies have selected patients on the basis of genetic factors or functional characteristics that might predict sensitivity to HSP90 inhibitors. Our data suggest that in certain cancers, such as those driven by mutant KRAS, the response to HSP90 inhibition is determined by their dependence on a single or a small number of client proteins, such as STK33, whose degradation cannot be compensated. Based on this observation, we hypothesize that the subset of patients who benefit from HSP90 inhibitors might be enriched for cases codependent on mutant KRAS and STK33. It will therefore be of interest to test tumor tissue from patients enrolled on clinical trials of these agents for the presence of KRAS mutations. Other examples of genetically defined cancers that appear to be hypersensitive to HSP90 inhibition include *ERBB2*-amplified breast cancer (Modi et al., 2007, 2011) and lung adenocarcinomas driven by the *EML4-ALK* fusion gene (Sequist et al., 2010; Normant et al., 2011). Thus, maximizing the clinical utility of HSP90 inhibitors as anticancer agents will require detailed knowledge of tumor genotypes and their associated phenotypic dependencies, illustrating the importance of combining structural and functional cancer genome efforts (Boehm and Hahn, 2011).

Despite promising preclinical data, several HSP90 inhibitors have shown limited efficacy as monotherapy in phase 2 trials of patients with epithelial and hematopoietic malignancies (Barginear et al., 2008; Mahalingam et al., 2009; Trepel et al., 2010). This highlights several challenges, in addition to choosing the right indication, that may complicate the rational clinical development of HSP90 inhibitors, including redundancy between signaling pathways, influences of the tumor microenvironment, and inefficient inhibition of intratumoral HSP90 activity (Workman et al., 2007; Trepel et al., 2010). Nevertheless, our findings demonstrate that HSP90 inhibitors are capable of inducing apoptosis in mutant KRAS-driven cancer cells by targeting their intrinsic dependence on STK33. We believe that this context-specific property of HSP90-targeted agents may best be exploited when coupled with conventional cytotoxic drugs or newer molecular cancer therapeutics, a strategy that has been successfully used in patients with multiple myeloma and ERBB2-positive breast cancer (Modi et al., 2007, 2011; Richardson et al., 2011).

In conclusion, the identification of STK33 as a new HSP90 client provides a rationale for targeting mutant KRAS-driven cancers, which are notoriously difficult to treat, in a genetically informed way. Of note, the potential value of such a personalized therapeutic approach in patients could be assessed immediately given that several HSP90 inhibitors are currently in clinical development. Finally, at such time as efforts to develop STK33 inhibitors are complicated by incomplete understanding of the specific properties of STK33 that are relevant to KRAS-mediated oncogenesis, HSP90 inhibition provides an alternative means to invoke complete loss of STK33 function for therapeutic benefit.

MATERIALS AND METHODS

Cell lines and inhibitors. Cell lines were maintained under standard conditions. PU-H71, 17-AAG, and MG-132 for in vitro studies were obtained from Sigma-Aldrich. PU-H71 for injection into mice was synthesized as reported (Caldas-Lopes et al., 2009). Bortezomib was obtained from LC Laboratories.

Plasmids, transfection, and lentiviral transduction. *STK33* and *BAG2* cDNAs were obtained from Open Biosystems. *RAF1* and *AKT1* cDNAs were obtained from W. Hahn and D. Root through Addgene (ID 23752 and 23832). Epitope tags were attached by PCR amplification. cDNAs were cloned into the pLenti6.2/V5-DEST lentiviral expression vector using Gateway Technology (Invitrogen). Xpress-tagged *USP5* and *USP15* cDNAs in the pcDNA4c vector were obtained from P. Howley through Addgene (ID 24744 and 23216). RNAi experiments were performed using pLKO.1 lentiviral shRNA vectors obtained from the TRC-Hs 1.0 (Human) shRNA library through Open Biosystems (shSTK33-1, TRCN0000002077; shSTK33-2, TRCN0000002079; shSTK33-3, TRCN0000002081; shHSP90A, TRCN0000001025; shHSP90B, TRCN0000008748; shBAG2-1, TRCN0000033590; shBAG-2, TRCN0000033591; shHERC2, TRCN0000118376; shRAF1, TRCN0000001067; shAKT1-1, TRCN0000039794; shAKT1-2, TRCN0000039797). For transient expression, cDNAs were transfected into 293T cells. Generation of viral supernatants and viral transduction were performed as described previously (Scholl et al., 2009).

Mass spectrometry. Whole-cell protein extracts were prepared using lysis buffer containing 20 mM Tris-HCl, 150 mM NaCl, 1 mM EDTA, 10% glycerol, and 0.5% NP-40 supplemented with Protease Arrest (G-Biosciences) and Phosphatase Inhibitor Cocktails 1 and 2 (Sigma-Aldrich). Protein extracts (9 mg BT-20; 17 mg MDA-MB-231) were precleared with 150 µl packed mouse IgG-Agarose (Sigma-Aldrich) for 1 h, and supernatants were incubated overnight with 150 µl packed Anti-FLAG M2 Affinity Gel beads (Sigma-Aldrich). Beads were washed five times in lysis buffer, and bound proteins were eluted using 3× FLAG Peptide (Sigma-Aldrich). Eluted proteins were concentrated with Microcon YM-10 centrifugal filter columns (Millipore) and separated by SDS-PAGE on a 4–12% gel. After staining of the gel with colloidal blue (Invitrogen), each lane was excised and cut into 10 equally sized pieces that were rinsed with HPLC water, followed by two washes in 50% acetonitrile. Peptides within each gel piece were sequenced at the Harvard Microchemistry and Proteomics Analysis Facility by microcapillary reverse-phase HPLC nanoelectrospray tandem mass spectrometry (µLC/MS/MS) on a LTQ-Orbitrap mass spectrometer (Thermo Fisher Scientific).

IP and Western blot analysis. Whole-cell protein extracts for IP and direct Western blotting were prepared using IP-lysis buffer containing 10 mM Tris-HCl, 5 mM EDTA, 50 mM NaCl, 50 mM NaF, and 1% Triton-X100 supplemented with Complete Protease Inhibitor Cocktail Tablets (Roche). Insoluble fractions were prepared with buffer containing 2% SDS and subjected to 16 cycles of sonification (30 s). Soluble fractions were prepared using IP-lysis buffer. Protein extracts (50–100 µg) were subjected to SDS-PAGE and transferred to nitrocellulose membranes (Whatman). Membranes were blocked using 5% dry milk in PBS containing 0.2% Tween-20, followed by incubation with primary and HRP-linked secondary antibodies (GE Healthcare). For coIP, protein extracts (1–2 mg) were incubated with 2 µg of antibody and Protein G–Sepharose (GE Healthcare) at 4°C. Immobilized proteins were washed three times, resuspended in Laemmli buffer, and subjected to SDS-PAGE and Western blotting. Bands were quantified by densitometric analysis using ImageJ software (http://imagej.nih.gov/ij). The following antibodies were used: anti-FLAG M2 Affinity Gel, anti–β-actin (Sigma-Aldrich); anti-PARP, anti-caspase 9 (human-specific), anti-RAF1, and anti-AKT1 (Cell Signaling Technology); anti-STK33 (clone 4F7; Abnova); anti-HA (clone Y-11), anti-CDC37 (clone H-271), anti-HSP90α/β (clone H-114), anti-HSP90β (clone D-19), anti–K-Ras-2B (clone C-19), anti-Neu (clone H-200), and anti-FLT3 (clone C-20; Santa Cruz Biotechnology); anti-BAG2 (clone EPR3567; Epitomics); anti-HERC2 (clone 17; BD); anti-ubiquitin (EMD); anti-Xpress (Invitrogen); and anti-HSP90α (AB3466; Millipore).

Cell viability and proliferation assays and analysis of caspase 9 activity. Viability and proliferation of cell lines incubated with PU-H71 were determined using the CellTiter $96AQ_{ueous}$ One Solution Proliferation Assay (Promega). Caspase 9 activity was measured using the Caspase-Glo 9 Assay (Promega).

CAM assay and IHC. HCT-116, Caco-2, and MDA-MB-231 cells (1.3×10^6 each) were deposited within 5-mm silicon rings on the surface of chicken CAM 8 d after fertilization. 17-AAG (5 µM) and PU-H71 (1 µM) were administered 24 and 48 h after implantation, and xenograft tumors were harvested after 72 h. Tumor areas were measured using ImageJ software. Formalin-fixed tumors were embedded in paraffin, and IHC was performed using the following antibodies: anti-STK33 (1:100; clone 4F7; Abnova) and anti-FLAG M2 (1:1,000; Sigma-Aldrich). Apoptotic cells were detected by TUNEL using the In Situ Cell Death Detection kit, POD (Roche) and quantified by counting >600 cells from at least four microscopic fields.

Mouse xenotransplantation experiments. HCT-116, SW-480, Caco-2, and Colo-320HSR colon cancer cells (8×10^6 each) were injected s.c. into the flanks of nude mice (NMRI-nu [nu/nu]; Janvier), and tumor formation was monitored. For each cell line, mice were separated into a treatment group and a control group (four to seven mice each) with comparable average tumor sizes. Mice in the treatment group received 75 mg per kg body weight PU-H71 i.p. three times per wk, and mice in the control group received PBS. Tumor size was measured weekly, and mice were sacrificed when tumors reached the maximum size permitted by the institutionally approved protocol or after 3 wk. IHC of tumors was performed as described for CAM experiments in the previous section. For Western blot analysis, tumors were frozen in liquid nitrogen and disintegrated, and protein extracts were prepared using IP-lysis buffer. Approval for the use of animals in this study was granted by the Animal Care and Use Committee at the Regierungspräsidium Tübingen under protocol number 1030.

HSP90 inhibitor treatment of primary human colon cancer cells. Tissue specimens from primary human colon carcinomas were obtained under an Institutional Review Board-approved protocol following written informed consent. Sphere cultures were established as previously described (Kreso and O'Brien, 2008) and maintained in DME/F-12 supplemented with 0.6% glucose, 1% penicillin/streptomycin, 2 mM L-glutamine, 4 µg/ml heparin, 5 mM Hepes, 4 mg/ml BSA, 10 ng/ml FGF basic (R&D Systems), and 20 ng/ml EGF (R&D Systems). For functional studies, tumor spheres were mechanically dissociated, and cells were seeded in 96-well plates according to the basal ATP level of the different patient cultures (SC-01 and SC-02, 400 cells; SC-03 and SC-04, 1,500 cells; SC-05, 3,000 cells). PU-H71 or PBS was added after 24 h, and cell viability was determined using the CellTiter-Glo Luminescent Cell Viability Assay (Promega) after 48 h.

Statistical analysis. All results were confirmed in at least one independent experiment, although typically more (as indicated in figure legends). Statistical significance was assessed with an unpaired Student's *t* test using GraphPad Prism Version 5.0a (GraphPad Software).

The authors thank Martina Schneider for technical assistance, and Gary Gilliland, Steven Lane, Stephen Sykes, and Thorsten Zenz for their advice and critical review of the manuscript.

This study was supported by the German Cancer Aid and by an Emmy Noether Fellowship from the German Research Foundation (to C. Scholl). J. Ellegast was supported by a Young Investigator Fellowship from the Medical Faculty of Ulm University. G. Chiosis is supported in part by National Institutes of Health grant 1R01-CA-155226-01. H. Glimm is supported in part by grants from the German Research Foundation (KFO 227) and the Baden-Württemberg Stiftung.

The authors have no conflicting financial interests.

Submitted: 8 September 2011
Accepted: 15 February 2012

REFERENCES

Babij, C., Y. Zhang, R.J. Kurzeja, A. Munzli, A. Shehabeldin, M. Fernando, K. Quon, P.D. Kassner, A.A. Ruefli-Brasse, V.J. Watson, et al. 2011. STK33 kinase activity is nonessential in KRAS-dependent cancer cells. *Cancer Res.* 71:5818–5826. http://dx.doi.org/10.1158/0008-5472.CAN-11-0778

Banerji, U., A. O'Donnell, M. Scurr, S. Pacey, S. Stapleton, Y. Asad, L. Simmons, A. Maloney, F. Raynaud, M. Campbell, et al. 2005. Phase I pharmacokinetic and pharmacodynamic study of 17-allylamino, 17-demethoxygeldanamycin in patients with advanced malignancies. *J. Clin. Oncol.* 23:4152–4161. http://dx.doi.org/10.1200/JCO.2005.00.612

Barbie, D.A., P. Tamayo, J.S. Boehm, S.Y. Kim, S.E. Moody, I.F. Dunn, A.C. Schinzel, P. Sandy, E. Meylan, C. Scholl, et al. 2009. Systematic RNA interference reveals that oncogenic KRAS-driven cancers require TBK1. *Nature.* 462:108–112. http://dx.doi.org/10.1038/nature08460

Bardelli, A., and S. Siena. 2010. Molecular mechanisms of resistance to cetuximab and panitumumab in colorectal cancer. *J. Clin. Oncol.* 28: 1254–1261. http://dx.doi.org/10.1200/JCO.2009.24.6116

Barginear, M.F., C. Van Poznak, N. Rosen, S. Modi, C.A. Hudis, and D.R. Budman. 2008. The heat shock protein 90 chaperone complex: an evolving therapeutic target. *Curr. Cancer Drug Targets.* 8:522–532. http://dx.doi.org/10.2174/156800908785699379

Boehm, J.S., and W.C. Hahn. 2011. Towards systematic functional characterization of cancer genomes. *Nat. Rev. Genet.* 12:487–498. http://dx.doi.org/10.1038/nrg3013

Caldas-Lopes, E., L. Cerchietti, J.H. Ahn, C.C. Clement, A.I. Robles, A. Rodina, K. Moulick, T. Taldone, A. Gozman, Y. Guo, et al. 2009. Hsp90 inhibitor PU-H71, a multimodal inhibitor of malignancy, induces complete responses in triple-negative breast cancer models. *Proc. Natl. Acad. Sci. USA*. 106:8368–8373. http://dx.doi.org/10.1073/pnas.0903392106

Cerchietti, L.C., E.C. Lopes, S.N. Yang, K. Hatzi, K.L. Bunting, L.A. Tsikitas, A. Mallik, A.I. Robles, J. Walling, L. Varticovski, et al. 2009. A purine scaffold Hsp90 inhibitor destabilizes BCL-6 and has specific antitumor activity in BCL-6-dependent B cell lymphomas. *Nat. Med.* 15:1369–1376. http://dx.doi.org/10.1038/nm.2059

Dai, Q., S.B. Qian, H.H. Li, H. McDonough, C. Borchers, D. Huang, S. Takayama, J.M. Younger, H.Y. Ren, D.M. Cyr, and C. Patterson. 2005. Regulation of the cytoplasmic quality control protein degradation pathway by BAG2. *J. Biol. Chem.* 280:38673–38681. http://dx.doi.org/10.1074/jbc.M507986200

de Bono, J.S., and A. Ashworth. 2010. Translating cancer research into targeted therapeutics. *Nature*. 467:543–549. http://dx.doi.org/10.1038/nature09339

Downward, J. 2003. Targeting RAS signalling pathways in cancer therapy. *Nat. Rev. Cancer.* 3:11–22. http://dx.doi.org/10.1038/nrc969

Druker, B.J. 2009. Perspectives on the development of imatinib and the future of cancer research. *Nat. Med.* 15:1149–1152. http://dx.doi.org/10.1038/nm1009-1149

Engelman, J.A., L. Chen, X. Tan, K. Crosby, A.R. Guimaraes, R. Upadhyay, M. Maira, K. McNamara, S.A. Perera, Y. Song, et al. 2008. Effective use of PI3K and MEK inhibitors to treat mutant Kras G12D and PIK3CA H1047R murine lung cancers. *Nat. Med.* 14:1351–1356. http://dx.doi.org/10.1038/nm.1890

George, P., P. Bali, P. Cohen, J. Tao, F. Guo, C. Sigua, A. Vishvanath, W. Fiskus, A. Scuto, S. Annavarapu, et al. 2004. Cotreatment with 17-allylamino-demethoxygeldanamycin and FLT-3 kinase inhibitor PKC412 is highly effective against human acute myelogenous leukemia cells with mutant FLT-3. *Cancer Res.* 64:3645–3652. http://dx.doi.org/10.1158/0008-5472.CAN-04-0006

Gorre, M.E., K. Ellwood-Yen, G. Chiosis, N. Rosen, and C.L. Sawyers. 2002. BCR-ABL point mutants isolated from patients with imatinib mesylate-resistant chronic myeloid leukemia remain sensitive to inhibitors of the BCR-ABL chaperone heat shock protein 90. *Blood.* 100:3041–3044. http://dx.doi.org/10.1182/blood-2002-05-1361

Gupta, S., A.R. Ramjaun, P. Haiko, Y. Wang, P.H. Warne, B. Nicke, E. Nye, G. Stamp, K. Alitalo, and J. Downward. 2007. Binding of ras to phosphoinositide 3-kinase p110α is required for ras-driven tumorigenesis in mice. *Cell.* 129:957–968. http://dx.doi.org/10.1016/j.cell.2007.03.051

Halilovic, E., Q.B. She, Q. Ye, R. Pagliarini, W.R. Sellers, D.B. Solit, and N. Rosen. 2010. PIK3CA mutation uncouples tumor growth and cyclin D1 regulation from MEK/ERK and mutant KRAS signaling. *Cancer Res.* 70:6804–6814. http://dx.doi.org/10.1158/0008-5472.CAN-10-0409

Hudis, C.A. 2007. Trastuzumab—mechanism of action and use in clinical practice. *N. Engl. J. Med.* 357:39–51. http://dx.doi.org/10.1056/NEJMra043186

International Cancer Genome Consortium. 2010. International network of cancer genome projects. *Nature*. 464:993–998. http://dx.doi.org/10.1038/nature08987

Karnoub, A.E., and R.A. Weinberg. 2008. Ras oncogenes: split personalities. *Nat. Rev. Mol. Cell Biol.* 9:517–531. http://dx.doi.org/10.1038/nrm2438

Kim, Y.S., S.V. Alarcon, S. Lee, M.-J. Lee, G. Giaccone, L. Neckers, and J.B. Trepel. 2009. Update on Hsp90 inhibitors in clinical trial. *Curr. Top. Med. Chem.* 9:1479–1492. http://dx.doi.org/10.2174/156802609789895728

Kreso, A., and C.A. O'Brien. 2008. Colon cancer stem cells. *Curr. Protoc. Stem Cell Biol.* Chapter 3:Unit 3 1.

Lim, K.H., and C.M. Counter. 2005. Reduction in the requirement of oncogenic Ras signaling to activation of PI3K/AKT pathway during tumor maintenance. *Cancer Cell.* 8:381–392. http://dx.doi.org/10.1016/j.ccr.2005.10.014

Luo, J., M.J. Emanuele, D. Li, C.J. Creighton, M.R. Schlabach, T.F. Westbrook, K.-K. Wong, and S.J. Elledge. 2009. A genome-wide RNAi screen identifies multiple synthetic lethal interactions with the Ras oncogene. *Cell.* 137:835–848. http://dx.doi.org/10.1016/j.cell.2009.05.006

Luo, T., K. Masson, J.D. Jaffe, W. Silkworth, N.T. Ross, C.A. Scherer, C. Scholl, S. Fröhling, S.A. Carr, A.M. Stern, et al. 2012. STK33 kinase inhibitor BRD-8899 has no effect on KRAS-dependent cancer cell viability. *Proc. Natl. Acad. Sci. USA*. 109:2680–2685. http://www.ncbi.nlm.nih.gov/pubmed/22323609

Mahalingam, D., R. Swords, J.S. Carew, S.T. Nawrocki, K. Bhalla, and F.J. Giles. 2009. Targeting HSP90 for cancer therapy. *Br. J. Cancer.* 100:1523–1529. http://dx.doi.org/10.1038/sj.bjc.6605066

Maloney, A., P.A. Clarke, S. Naaby-Hansen, R. Stein, J.O. Koopman, A. Akpan, A. Yang, M. Zvelebil, R. Cramer, L. Stimson, et al. 2007. Gene and protein expression profiling of human ovarian cancer cells treated with the heat shock protein 90 inhibitor 17-allylamino-17-demethoxygeldanamycin. *Cancer Res.* 67:3239–3253. http://dx.doi.org/10.1158/0008-5472.CAN-06-2968

Malumbres, M., and M. Barbacid. 2003. RAS oncogenes: the first 30 years. *Nat. Rev. Cancer.* 3:459–465. http://dx.doi.org/10.1038/nrc1097

Marubayashi, S., P. Koppikar, T. Taldone, O. Abdel-Wahab, N. West, N. Bhagwat, E. Caldas-Lopes, K.N. Ross, M. Gönen, A. Gozman, et al. 2010. HSP90 is a therapeutic target in JAK2-dependent myeloproliferative neoplasms in mice and humans. *J. Clin. Invest.* 120:3578–3593. http://dx.doi.org/10.1172/JCI42442

Mimnaugh, E.G., C. Chavany, and L. Neckers. 1996. Polyubiquitination and proteasomal degradation of the p185c-erbB-2 receptor protein-tyrosine kinase induced by geldanamycin. *J. Biol. Chem.* 271:22796–22801. http://dx.doi.org/10.1074/jbc.271.9.4974

Modi, S., A.T. Stopeck, M.S. Gordon, D. Mendelson, D.B. Solit, R. Bagatell, W. Ma, J. Wheler, N. Rosen, L. Norton, et al. 2007. Combination of trastuzumab and tanespimycin (17-AAG, KOS-953) is safe and active in trastuzumab-refractory HER-2 overexpressing breast cancer: a phase I dose-escalation study. *J. Clin. Oncol.* 25:5410–5417. http://dx.doi.org/10.1200/JCO.2007.11.7960

Modi, S., A.T. Stopeck, H.M. Linden, D.B. Solit, S. Chandarlapaty, N. Rosen, G. D'Andrea, M.N. Dickler, M.E. Moynahan, S. Sugarman, et al. 2011. HSP90 inhibition is effective in breast cancer: a phase II trial of tanespimycin (17-AAG) plus trastuzumab in patients with HER2-positive metastatic breast cancer progressing on trastuzumab. *Clin. Cancer Res.* 17:5132–5139. http://dx.doi.org/10.1158/1078-0432.CCR-11-0072

Normant, E., G. Paez, K.A. West, A.R. Lim, K.L. Slocum, C. Tunkey, J. McDougall, A.A. Wylie, K. Robison, K. Caliri, et al. 2011. The Hsp90 inhibitor IPI-504 rapidly lowers EML4-ALK levels and induces tumor regression in ALK-driven NSCLC models. *Oncogene.* 30:2581–2586. http://dx.doi.org/10.1038/onc.2010.625

Picard, D. 2002. Heat-shock protein 90, a chaperone for folding and regulation. *Cell. Mol. Life Sci.* 59:1640–1648. http://dx.doi.org/10.1007/PL00012491

Puyol, M., A. Martín, P. Dubus, F. Mulero, P. Pizcueta, G. Khan, C. Guerra, D. Santamaría, and M. Barbacid. 2010. A synthetic lethal interaction between K-Ras oncogenes and Cdk4 unveils a therapeutic strategy for non-small cell lung carcinoma. *Cancer Cell.* 18:63–73. http://dx.doi.org/10.1016/j.ccr.2010.05.025

Richardson, P.G., C.S. Mitsiades, J.P. Laubach, S. Lonial, A.A. Chanan-Khan, and K.C. Anderson. 2011. Inhibition of heat shock protein 90 (HSP90) as a therapeutic strategy for the treatment of myeloma and other cancers. *Br. J. Haematol.* 152:367–379. http://dx.doi.org/10.1111/j.1365-2141.2010.08360.x

Roberts, P.J., and C.J. Der. 2007. Targeting the Raf-MEK-ERK mitogen-activated protein kinase cascade for the treatment of cancer. *Oncogene.* 26:3291–3310. http://dx.doi.org/10.1038/sj.onc.1210422

Roberts, P.J., T.E. Stinchcombe, C.J. Der, and M.A. Socinski. 2010. Personalized medicine in non-small-cell lung cancer: is KRAS a useful marker in selecting patients for epidermal growth factor receptor-targeted therapy? *J. Clin. Oncol.* 28:4769–4777. http://dx.doi.org/10.1200/JCO.2009.27.4365

Sawai, A., S. Chandarlapaty, H. Greulich, M. Gonen, Q. Ye, C.L. Arteaga, W. Sellers, N. Rosen, and D.B. Solit. 2008. Inhibition of Hsp90 down-regulates mutant epidermal growth factor receptor (EGFR) expression and sensitizes EGFR mutant tumors to paclitaxel. *Cancer Res.* 68:589–596. http://dx.doi.org/10.1158/0008-5472.CAN-07-1570

Scholl, C., S. Fröhling, I.F. Dunn, A.C. Schinzel, D.A. Barbie, S.Y. Kim, S.J. Silver, P. Tamayo, R.C. Wadlow, S. Ramaswamy, et al. 2009. Synthetic lethal interaction between oncogenic KRAS dependency and

STK33 suppression in human cancer cells. *Cell.* 137:821–834. http://dx.doi.org/10.1016/j.cell.2009.03.017

Sequist, L.V., S. Gettinger, N.N. Senzer, R.G. Martins, P.A. Jänne, R. Lilenbaum, J.E. Gray, A.J. Iafrate, R. Katayama, N. Hafeez, et al. 2010. Activity of IPI-504, a novel heat-shock protein 90 inhibitor, in patients with molecularly defined non-small-cell lung cancer. *J. Clin. Oncol.* 28:4953–4960. http://dx.doi.org/10.1200/JCO.2010.30.8338

Sharma, S.V., D.W. Bell, J. Settleman, and D.A. Haber. 2007. Epidermal growth factor receptor mutations in lung cancer. *Nat. Rev. Cancer.* 7:169–181. http://dx.doi.org/10.1038/nrc2088

Singh, A., P. Greninger, D. Rhodes, L. Koopman, S. Violette, N. Bardeesy, and J. Settleman. 2009. A gene expression signature associated with "K-Ras addiction" reveals regulators of EMT and tumor cell survival. *Cancer Cell.* 15:489–500. http://dx.doi.org/10.1016/j.ccr.2009.03.022

Sos, M.L., K. Michel, T. Zander, J. Weiss, P. Frommolt, M. Peifer, D. Li, R. Ullrich, M. Koker, F. Fischer, et al. 2009. Predicting drug susceptibility of non-small cell lung cancers based on genetic lesions. *J. Clin. Invest.* 119:1727–1740. http://dx.doi.org/10.1172/JCI37127

Stratton, M.R., P.J. Campbell, and P.A. Futreal. 2009. The cancer genome. *Nature.* 458:719–724. http://dx.doi.org/10.1038/nature07943

Taipale, M., D.F. Jarosz, and S. Lindquist. 2010. HSP90 at the hub of protein homeostasis: emerging mechanistic insights. *Nat. Rev. Mol. Cell Biol.* 11:515–528. http://dx.doi.org/10.1038/nrm2918

Taldone, T., and G. Chiosis. 2009. Purine-scaffold Hsp90 inhibitors. *Curr. Top. Med. Chem.* 9:1436–1446. http://dx.doi.org/10.2174/156802609789895737

Taldone, T., A. Gozman, R. Maharaj, and G. Chiosis. 2008. Targeting Hsp90: small-molecule inhibitors and their clinical development. *Curr. Opin. Pharmacol.* 8:370–374. http://dx.doi.org/10.1016/j.coph.2008.06.015

Trepel, J., M. Mollapour, G. Giaccone, and L. Neckers. 2010. Targeting the dynamic HSP90 complex in cancer. *Nat. Rev. Cancer.* 10:537–549. http://dx.doi.org/10.1038/nrc2887

Vicent, S., R. Chen, L.C. Sayles, C. Lin, R.G. Walker, A.K. Gillespie, A. Subramanian, G. Hinkle, X. Yang, S. Saif, et al. 2010. Wilms tumor 1 (WT1) regulates KRAS-driven oncogenesis and senescence in mouse and human models. *J. Clin. Invest.* 120:3940–3952. http://dx.doi.org/10.1172/JCI44165

Wang, Y., V.N. Ngo, M. Marani, Y. Yang, G. Wright, L.M. Staudt, and J. Downward. 2010. Critical role for transcriptional repressor Snail2 in transformation by oncogenic RAS in colorectal carcinoma cells. *Oncogene.* 29:4658–4670. http://dx.doi.org/10.1038/onc.2010.218

Wee, S., Z. Jagani, K.X. Xiang, A. Loo, M. Dorsch, Y.M. Yao, W.R. Sellers, C. Lengauer, and F. Stegmeier. 2009. PI3K pathway activation mediates resistance to MEK inhibitors in KRAS mutant cancers. *Cancer Res.* 69:4286–4293. http://dx.doi.org/10.1158/0008-5472.CAN-08-4765

Weiss, W.A., S.S. Taylor, and K.M. Shokat. 2007. Recognizing and exploiting differences between RNAi and small-molecule inhibitors. *Nat. Chem. Biol.* 3:739–744. http://dx.doi.org/10.1038/nchembio1207-739

West, K.A., N. Hafeez, J. Mac Dougall, E. Normant, V. Palombella, and C. Fritz. 2011. Abstract 2827: Activity of the proprietary Hsp90 inhibitor IPI-493 in models of colorectal cancer correlates with RAS pathway activation. *Cancer Res.* 71:2827.

Wong, K., M. Koczywas, J.W. Goldman, E.H. Paschold, L. Horn, J.M. Lufkin, R.K. Blackman, F. Teofilovici, G. Shapiro, and M.A. Socinski. 2011. An open-label phase II study of the Hsp90 inhibitor ganetespib (STA-9090) as monotherapy in patients with advanced non-small cell lung cancer (NSCLC). *ASCO Meeting Abstracts.* 29:7500.

Workman, P., F. Burrows, L. Neckers, and N. Rosen. 2007. Drugging the cancer chaperone HSP90: combinatorial therapeutic exploitation of oncogene addiction and tumor stress. *Ann. N. Y. Acad. Sci.* 1113:202–216. http://dx.doi.org/10.1196/annals.1391.012

Yu, K., L. Toral-Barza, C. Shi, W.G. Zhang, and A. Zask. 2008. Response and determinants of cancer cell susceptibility to PI3K inhibitors: combined targeting of PI3K and Mek1 as an effective anticancer strategy. *Cancer Biol. Ther.* 7:307–315.

Zhang, H., D. Chung, Y.C. Yang, L. Neely, S. Tsurumoto, J. Fan, L. Zhang, M. Biamonte, J. Brekken, K. Lundgren, and F. Burrows. 2006. Identification of new biomarkers for clinical trials of Hsp90 inhibitors. *Mol. Cancer Ther.* 5:1256–1264. http://dx.doi.org/10.1158/1535-7163.MCT-05-0537